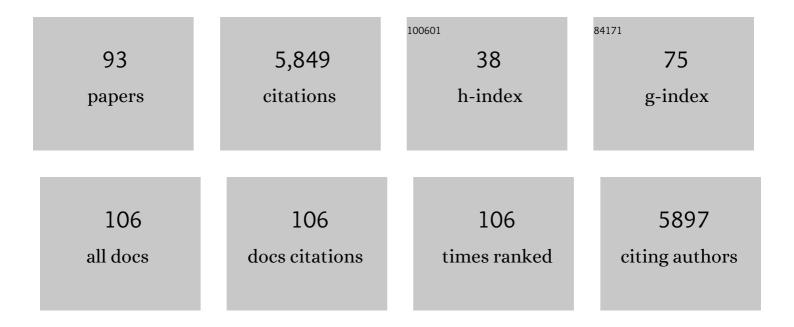
## Heather C Allen

List of Publications by Year in descending order

Source: https://exaly.com/author-pdf/8674946/publications.pdf Version: 2024-02-01



#	Article	IF	CITATIONS
1	La3+ and Y3+ interactions with the carboxylic acid moiety at the liquid/vapor interface: Identification of binding complexes, charge reversal, and detection limits. Journal of Colloid and Interface Science, 2022, 608, 2169-2180.	5.0	17
2	Recognition competes with hydration in anion-triggered monolayer formation of cyanostar supra-amphiphiles at aqueous interfaces. Chemical Science, 2022, 13, 4283-4294.	3.7	7
3	Phase State and Thermodynamic Properties of Proxy Sea Spray Aerosol Interfaces Derived from Temperature-Dependent Equilibrium Spreading Pressure. ACS Earth and Space Chemistry, 2022, 6, 1563-1573.	1.2	1
4	Discerning Poly- and Monosaccharide Enrichment Mechanisms: Alginate and Glucuronate Adsorption to a Stearic Acid Sea Surface Microlayer. ACS Earth and Space Chemistry, 2022, 6, 1581-1595.	1.2	6
5	Vibrational exciton delocalization precludes the use of infrared intensities as proxies for surfactant accumulation on aqueous surfaces. Chemical Science, 2021, 12, 8320-8332.	3.7	3
6	Calcium bridging drives polysaccharide co-adsorption to a proxy sea surface microlayer. Physical Chemistry Chemical Physics, 2021, 23, 16401-16416.	1.3	8
7	Insight into the Ionizing Surface Potential Method and Aqueous Sodium Halide Surfaces. Langmuir, 2021, 37, 7863-7874.	1.6	5
8	Functional Group Identification for FTIR Spectra Using Image-Based Machine Learning Models. Analytical Chemistry, 2021, 93, 9711-9718.	3.2	51
9	Zinc–Carboxylate Binding in Mixed Octadecanoic Acid and Octadecanol Monolayers on Proxy Seawater Solution Surfaces. ACS Earth and Space Chemistry, 2021, 5, 2947-2956.	1.2	4
10	Circuit Analysis of Ionizing Surface Potential Measurements of Electrolyte Solutions. Journal of the Electrochemical Society, 2021, 168, 016507.	1.3	8
11	Role of Hydration in Magnesium versus Calcium Ion Pairing with Carboxylate: Solution and the Aqueous Interface. Journal of Physical Chemistry B, 2021, 125, 11308-11319.	1.2	13
12	Hydration and Hydrogen Bond Order of Octadecanoic Acid and Octadecanol Films on Water at 21 and 1 °C. Journal of Physical Chemistry A, 2021, 125, 10065-10078.	1.1	8
13	Sodium Drives Interfacial Equilibria for Semi-Soluble Phosphoric and Phosphonic Acids of Model Sea Spray Aerosol Surfaces. ACS Earth and Space Chemistry, 2020, 4, 1549-1557.	1.2	7
14	Relating Structure and Ice Nucleation of Mixed Surfactant Systems Relevant to Sea Spray Aerosol. Journal of Physical Chemistry A, 2020, 124, 8806-8821.	1.1	15
15	Molecular Recognition and Hydration Energy Mismatch Combine To Inform Ion Binding Selectivity at Aqueous Interfaces. Journal of Physical Chemistry A, 2020, 124, 10171-10180.	1.1	10
16	The Ocean's Elevator: Evolution of the Air–Seawater Interface during a Small-Scale Algal Bloom. ACS Earth and Space Chemistry, 2020, 4, 2347-2357.	1.2	11
17	One-Pot Aldol Cascade for the Preparation of Isospiropyrans, Flavylium Salts, and bis-Spiropyrans. Journal of Organic Chemistry, 2020, 85, 8013-8020.	1.7	2
18	Thermodynamic Signatures of the Origin of <i>Anti</i> Hofmeister Selectivity for Phosphate at Aqueous Interfaces. Journal of Physical Chemistry A, 2020, 124, 5621-5630.	1.1	23

#	Article	IF	CITATIONS
19	Structural Effects of Cation Binding to DPPC Monolayers. Langmuir, 2020, 36, 15258-15269.	1.6	8
20	Hydration of ferric chloride and nitrate in aqueous solutions: water-mediated ion pairing revealed by Raman spectroscopy. Physical Chemistry Chemical Physics, 2019, 21, 19172-19180.	1.3	9
21	Iron(III) Speciation Observed at Aqueous and Glycerol Surfaces: Vibrational Sum Frequency and X-ray. Journal of the American Chemical Society, 2019, 141, 13525-13535.	6.6	27
22	Molecular-level origin of the carboxylate head group response to divalent metal ion complexation at the air–water interface. Proceedings of the National Academy of Sciences of the United States of America, 2019, 116, 14874-14880.	3.3	37
23	An easily accessible isospiropyran switch. Organic and Biomolecular Chemistry, 2019, 17, 9124-9128.	1.5	2
24	Biogeochemical Equation of State for the Sea-Air Interface. Atmosphere, 2019, 10, 230.	1.0	7
25	Interfacial Supramolecular Structures of Amphiphilic Receptors Drive Aqueous Phosphate Recognition. Journal of the American Chemical Society, 2019, 141, 7876-7886.	6.6	42
26	Thermodynamic <i>versus</i> non-equilibrium stability of palmitic acid monolayers in calcium-enriched sea spray aerosol proxy systems. Physical Chemistry Chemical Physics, 2018, 20, 16320-16332.	1.3	21
27	Presence and persistence of a highly ordered lipid phase state in the avian stratum corneum. Journal of Experimental Biology, 2018, 221, .	0.8	3
28	Effect of pH and Salt on Surface p <i>K</i> <sub>a</sub> of Phosphatidic Acid Monolayers. Langmuir, 2018, 34, 530-539.	1.6	41
29	Collapse Mechanisms of Nascent and Aged Sea Spray Aerosol Proxy Films. Atmosphere, 2018, 9, 503.	1.0	13
30	Trace Metal Enrichment Driven by Phosphate Functional Group Binding Selectivity. Journal of Geophysical Research: Oceans, 2018, 123, 5286-5297.	1.0	7
31	Vibrational Spectroscopy of Gas–Liquid Interfaces. , 2018, , 105-133.		8
32	Arginine–Phosphate Recognition Enhanced in Phospholipid Monolayers at Aqueous Interfaces. Journal of Physical Chemistry C, 2018, 122, 26362-26371.	1.5	29
33	Preface: Special Topic on Ions in Water. Journal of Chemical Physics, 2018, 148, 222501.	1.2	1
34	Bulk Contributions Modulate the Sum-Frequency Generation Spectra of Water on Model Sea-Spray Aerosols. CheM, 2018, 4, 1629-1644.	5.8	69
35	Sodium–carboxylate contact ion pair formation induces stabilization of palmitic acid monolayers at high pH. Physical Chemistry Chemical Physics, 2017, 19, 10481-10490.	1.3	42
36	Surface pK <sub>a</sub> of octanoic, nonanoic, and decanoic fatty acids at the air–water interface: applications to atmospheric aerosol chemistry. Physical Chemistry Chemical Physics, 2017, 19, 26551-26558.	1.3	80

#	Article	IF	CITATIONS
37	Solvent-Shared Ion Pairs at the Air–Solution Interface of Magnesium Chloride and Sulfate Solutions Revealed by Sum Frequency Spectroscopy and Molecular Dynamics Simulations. Journal of Physical Chemistry A, 2017, 121, 6450-6459.	1.1	26
38	Interfacial properties of avian stratum corneum monolayers investigated by Brewster angle microscopy and vibrational sum frequency generation. Chemistry and Physics of Lipids, 2017, 208, 1-9.	1.5	7
39	Surface Potential of DPPC Monolayers on Concentrated Aqueous Salt Solutions. Journal of Physical Chemistry B, 2016, 120, 2043-2052.	1.2	57
40	Cation effects on phosphatidic acid monolayers at various pH conditions. Chemistry and Physics of Lipids, 2016, 200, 24-31.	1.5	20
41	Surface organization of a DPPC monolayer on concentrated SrCl <sub>2</sub> and ZnCl <sub>2</sub> solutions. Physical Chemistry Chemical Physics, 2016, 18, 32345-32357.	1.3	38
42	Effect of cation enrichment on dipalmitoylphosphatidylcholine (DPPC) monolayers at the air-water interface. Journal of Colloid and Interface Science, 2016, 478, 353-364.	5.0	66
43	Organization of lipids in avian stratum corneum: Changes with temperature and hydration. Chemistry and Physics of Lipids, 2016, 195, 47-57.	1.5	10
44	Reduced Condensing and Ordering Effects by 7-Ketocholesterol and 5β,6β-Epoxycholesterol on DPPC Monolayers. Langmuir, 2015, 31, 9859-9869.	1.6	17
45	Solvation of Calcium–Phosphate Headgroup Complexes at the DPPC/Aqueous Interface. ChemPhysChem, 2015, 16, 3910-3915.	1.0	27
46	Interaction of <scp>l</scp> -Phenylalanine with a Phospholipid Monolayer at the Water–Air Interface. Journal of Physical Chemistry B, 2015, 119, 9038-9048.	1.2	47
47	Extracting Infrared Spectra of Protein Secondary Structures Using a Library of Protein Spectra and the Ramachandran Plot. Journal of Physical Chemistry B, 2015, 119, 13079-13092.	1.2	12
48	Relative Order of Sulfuric Acid, Bisulfate, Hydronium, and Cations at the Air–Water Interface. Journal of the American Chemical Society, 2015, 137, 13920-13926.	6.6	42
49	Lipid composition and molecular interactions change with depth in the avian stratum corneum to regulate cutaneous water loss. Journal of Experimental Biology, 2015, 218, 3032-3041.	0.8	11
50	Preface of John C. Hemminger Festschrift. Journal of Physical Chemistry C, 2014, 118, 28923-28923.	1.5	0
51	Surface Electric Fields of Aqueous Solutions of NH <sub>4</sub> NO <sub>3</sub> , Mg(NO <sub>3</sub> ) <sub>2</sub> , NaNO <sub>3</sub> , and LiNO <sub>3</sub> : Implications for Atmospheric Aerosol Chemistry. Journal of Physical Chemistry C, 2014, 118, 24941-24949.	1.5	37
52	Effects of laser excitation wavelength and optical mode on Raman spectra of human fresh colon, pancreas, and prostate tissues. Journal of Raman Spectroscopy, 2014, 45, 773-780.	1.2	9
53	Cation Effects on Interfacial Water Organization of Aqueous Chloride Solutions. I. Monovalent Cations: Li <sup>+</sup> , Na <sup>+</sup> , K <sup>+</sup> , and NH <sub>4</sub> <sup>+</sup> . Journal of Physical Chemistry B, 2014, 118, 8433-8440.	1.2	52
54	Influence of Salt Purity on Na <sup>+</sup> and Palmitic Acid Interactions. Journal of Physical Chemistry A, 2013, 117, 13412-13418.	1.1	18

#	Article	IF	CITATIONS
55	Impact of Salt Purity on Interfacial Water Organization Revealed by Conventional and Heterodyne-Detected Vibrational Sum Frequency Generation Spectroscopy. Journal of Physical Chemistry C, 2013, 117, 19577-19585.	1.5	38
56	Surface Prevalence of Perchlorate Anions at the Air/Aqueous Interface. Journal of Physical Chemistry Letters, 2013, 4, 4231-4236.	2.1	20
57	Salty Glycerol versus Salty Water Surface Organization: Bromide and Iodide Surface Propensities. Journal of Physical Chemistry A, 2013, 117, 6346-6353.	1.1	22
58	Palmitic Acid on Salt Subphases and in Mixed Monolayers of Cerebrosides: Application to Atmospheric Aerosol Chemistry. Atmosphere, 2013, 4, 315-336.	1.0	57
59	Organization of Water and Atmospherically Relevant Ions and Solutes: Vibrational Sum Frequency Spectroscopy at the Vapor/Liquid and Liquid/Solid Interfaces. Accounts of Chemical Research, 2012, 45, 110-119.	7.6	73
60	Hydrophobic Collapse of a Stearic Acid Film by Adsorbed I-Phenylalanine at the Air–Water Interface. Journal of Physical Chemistry B, 2012, 116, 7849-7857.	1.2	40
61	Bisulfate Dehydration at Air/Solution Interfaces Probed by Vibrational Sum Frequency Generation Spectroscopy. Journal of Physical Chemistry C, 2012, 116, 13161-13168.	1.5	15
62	Environmental Chemistry at Vapor/Water Interfaces: Insights from Vibrational Sum Frequency Generation Spectroscopy. Annual Review of Physical Chemistry, 2012, 63, 107-130.	4.8	133
63	From Conventional to Phase-Sensitive Vibrational Sum Frequency Generation Spectroscopy: Probing Water Organization at Aqueous Interfaces. Journal of Physical Chemistry Letters, 2012, 3, 3012-3028.	2.1	67
64	Electric Field Reversal of Na <sub>2</sub> SO <sub>4</sub> , (NH <sub>4</sub> ) <sub>2</sub> SO <sub>4</sub> , and Na <sub>2</sub> CO <sub>3</sub> Relative to CaCl <sub>2</sub> and NaCl at the Air/Aqueous Interface Revealed by Heterodyne Detected Phase-Sensitive Sum Frequency. Journal of Physical Chemistry Letters, 2011, 2, 2515-2520.	2.1	64
65	Interfacial Water Structure and Effects of Mg2+and Ca2+Binding to the COOH Headgroup of a Palmitic Acid Monolayer Studied by Sum Frequency Spectroscopy. Journal of Physical Chemistry B, 2011, 115, 34-40.	1.2	69
66	Direct comparison of phase-sensitive vibrational sum frequency generation with maximum entropy method: Case study of water. Journal of Chemical Physics, 2011, 135, 224701.	1.2	58
67	Surface organization of aqueous MgCl <sub>2</sub> and application to atmospheric marine aerosol chemistry. Proceedings of the National Academy of Sciences of the United States of America, 2010, 107, 6616-6621.	3.3	56
68	Vibrational Spectroscopic Characterization of Hematite, Maghemite, and Magnetite Thin Films Produced by Vapor Deposition. ACS Applied Materials & Interfaces, 2010, 2, 2804-2812.	4.0	652
69	Interfacial Water Structure Associated with Phospholipid Membranes Studied by Phase-Sensitive Vibrational Sum Frequency Generation Spectroscopy. Journal of the American Chemical Society, 2010, 132, 11336-11342.	6.6	341
70	Binding of Mg <sup>2+</sup> and Ca <sup>2+</sup> to Palmitic Acid and Deprotonation of the COOH Headgroup Studied by Vibrational Sum Frequency Generation Spectroscopy. Journal of Physical Chemistry B, 2010, 114, 17068-17076.	1.2	95
71	Incorporation and Exclusion of Long Chain Alkyl Halides in Fatty Acid Monolayers at the Airâ `Water Interface. Langmuir, 2010, 26, 18806-18816.	1.6	17
72	Effect of Magnesium Cation on the Interfacial Properties of Aqueous Salt Solutions. Journal of Physical Chemistry A, 2010, 114, 8359-8368.	1.1	26

#	Article	IF	CITATIONS
73	Na <sup>+</sup> and Ca <sup>2+</sup> Effect on the Hydration and Orientation of the Phosphate Group of DPPC at Air <i>â^²</i> Water and Air <i>â^²</i> Hydrated Silica Interfaces. Journal of Physical Chemistry B, 2010, 114, 9485-9495.	1.2	84
74	Shedding light on water structure at air–aqueous interfaces: ions, lipids, and hydration. Physical Chemistry Chemical Physics, 2009, 11, 5538.	1.3	112
75	Nitrate Anions and Ion Pairing at the Airâ^'Aqueous Interface. Journal of Physical Chemistry C, 2009, 113, 2082-2087.	1.5	39
76	lonic Binding of Na <sup>+</sup> versus K <sup>+</sup> to the Carboxylic Acid Headgroup of Palmitic Acid Monolayers Studied by Vibrational Sum Frequency Generation Spectroscopy. Journal of Physical Chemistry A, 2009, 113, 7383-7393.	1.1	117
77	Water Structure at the Airâ^'Aqueous Interface of Divalent Cation and Nitrate Solutions. Journal of Physical Chemistry B, 2009, 113, 4102-4110.	1.2	43
78	Aqueous divalent metal–nitrate interactions: hydration versus ion pairing. Physical Chemistry Chemical Physics, 2008, 10, 4793.	1.3	82
79	Uptake and Surface Reaction of Methanol by Sulfuric Acid Solutions Investigated by Vibrational Sum Frequency Generation and Raman Spectroscopies. Journal of Physical Chemistry A, 2008, 112, 7873-7880.	1.1	17
80	Dangling OD Confined in a Langmuir Monolayer. Journal of the American Chemical Society, 2007, 129, 14053-14057.	6.6	53
81	Observation of Hydronium Ions at the Airâ^'Aqueous Acid Interface:  Vibrational Spectroscopic Studies of Aqueous HCl, HBr, and HI. Journal of Physical Chemistry C, 2007, 111, 8814-8826.	1.5	131
82	Oxidation of oleic acid at air/liquid interfaces. Journal of Geophysical Research, 2007, 112, .	3.3	37
83	Vibrational Spectroscopic Studies of Aqueous Interfaces:  Salts, Acids, Bases, and Nanodrops. Chemical Reviews, 2006, 106, 1155-1175.	23.0	414
84	DPPC Langmuir Monolayer at the Airâ^'Water Interface:  Probing the Tail and Head Groups by Vibrational Sum Frequency Generation Spectroscopy. Langmuir, 2006, 22, 5341-5349.	1.6	274
85	New Insights into Lung Surfactant Monolayers Using Vibrational Sum Frequency Generation Spectroscopy. Photochemistry and Photobiology, 2006, 82, 1517-1529.	1.3	36
86	Airâ^'Liquid Interfaces of Aqueous Solutions Containing Ammonium and Sulfate:Â Spectroscopic and Molecular Dynamics Studies. Journal of Physical Chemistry B, 2005, 109, 8861-8872.	1.2	195
87	Unified Molecular Picture of the Surfaces of Aqueous Acid, Base, and Salt Solutions. Journal of Physical Chemistry B, 2005, 109, 7617-7623.	1.2	393
88	Methanol Reaction with Sulfuric Acid:  A Vibrational Spectroscopic Study. Journal of Physical Chemistry B, 2004, 108, 17666-17674.	1.2	34
89	Vibrational Spectroscopy of Aqueous Sodium Halide Solutions and Airâ^'Liquid Interfaces:  Observation of Increased Interfacial Depth. Journal of Physical Chemistry B, 2004, 108, 2252-2260.	1.2	460
90	Surface Studies of Aqueous Methanol Solutions by Vibrational Broad Bandwidth Sum Frequency Generation Spectroscopy. Journal of Physical Chemistry B, 2003, 107, 6343-6349.	1.2	132

#	Article	IF	CITATIONS
91	1-Methyl Naphthalene Reorientation at the Airâ^'Liquid Interface upon Water Saturation Studied by Vibrational Broad Bandwidth Sum Frequency Generation Spectroscopy. Journal of Physical Chemistry B, 2003, 107, 10823-10828.	1.2	16
92	Surface Structural Studies of Methanesulfonic Acid at Air /Aqueous Solution Interfaces Using Vibrational Sum Frequency Spectroscopyâ€. Journal of Physical Chemistry A, 2001, 105, 1649-1655.	1.1	88
93	The Analysis of Interference Effects in the Sum Frequency Spectra of Water Interfacesâ€. Journal of Physical Chemistry A, 2000, 104, 10220-10226.	1.1	107